Food Innovation and Advances

ARTICLE

Open Access

https://doi.org/10.48130/FIA-2023-0002

Food Innovation and Advances **2023**, 2(1):9–17

Isomerization and bioaccessibility of cypermethrin and fenpropathrin in Pacific oyster during simulated digestion as influenced by domestic cooking methods

Hangtao Xie[1], Yadan Jiao[1], Tian Li[1], Tuo Zhang[1,3], Yanyan Zheng[4], Yongkang Luo[1], Yuqing Tan[1], Chune Liu[2*] and Hui Hong[1,3*]

[1] *Beijing Laboratory for Food Quality and Safety, College of Food Science and Nutritional Engineering, China Agricultural University, Beijing 100083, China*
[2] *Institute of Yantai, China Agricultural University, Yantai 264670, Shandong, China*
[3] *Center of Food Colloids and Delivery for Functionality, College of Food Science and Nutritional Engineering, China Agricultural University, Beijing 100083, China*
[4] *Institute of Agri-food Processing and Nutrition, Beijing Academy of Agriculture and Forestry Sciences, Beijing 100097, China*
* Corresponding authors, E-mail: lchune@126.com; hhong@cau.edu.cn

Abstract

Pyrethroids can be ingested by humans through eating contaminated oysters, which is potentially harmful to health. This study aimed to investigate the effects of raw, steaming, and roasting on cypermethrin (CP) and fenpropathrin (FP) in oysters during simulated digestion. Results showed that the amount of released CP and FP was different from raw (CP: 0.617 μg·g^{-1}, FP: 0.266 μg·g^{-1}), steaming (CP: 0.498 μg·g^{-1}, FP: 0.660 μg·g^{-1}), and roasting (CP: 1.186 μg·g^{-1}, FP: 0.588 μg·g^{-1}) at the end of simulated digestion. The share of cis-CP and low-efficiency CP increased significantly ($p < 0.05$), and the share of high-efficiency trans-CP did not maintain a high level for a long time during simulated digestion. The fluorimetric titration and isothermal titration calorimetry confirmed that CP and FP could spontaneously interact with oyster actin, and CP could bind with oyster actin more tightly than FP. This study reveals that cooking methods affect the binding capacity of CP and FP to oyster tissues and influence the changes of CP and FP in oysters during digestion. Furthermore, the current study provides a reference for assessing the potential harm of pyrethroids in oysters to consumers.

Citation: Xie H, Jiao Y, Li T, Zhang T, Zheng Y, et al. 2023. Isomerization and bioaccessibility of cypermethrin and fenpropathrin in Pacific oyster during simulated digestion as influenced by domestic cooking methods. *Food Innovation and Advances* 2(1):9–17 https://doi.org/10.48130/FIA-2023-0002

INTRODUCTION

Synthetic pyrethroids are increasingly being used for pest control in agriculture and urban areas[1]. Compared with pesticides formerly used, such as organochlorine and organophosphorus pesticides, pyrethroids have higher insecticidal effects and lower toxicity to mammals. Nevertheless, pyrethroids widely exist in the natural environment due to improper usage[2,3], and these pyrethroids may enter the natural water through rainwater runoff[4,5]. Pyrethroids can cause severe damage to aquatic animals due to their accumulative effect and poor decomposition ability[6,7]. Cypermethrin (CP) and fenpropathrin (FP) are two representative pyrethroids widely used in agriculture, and their metabolites are commonly detected in human urine[8,9]. Although some toxicological studies showed that pyrethroids are less harmful to mammalian health than other pesticides previously used, several studies have found the potential toxicity of pyrethroids to human organs such as the nervous, immune, cardiovascular systems, and even the reproductive system[1,10].

Pyrethroids have many isomers, but there is only one kind of isomer with high insecticidal activity in many cases[11]. Furthermore, different isomers are degraded selectively *in vivo* or in the natural environment[12]. Using pyrethroids with multiple isomers seems unreasonable because many of the isomers are of low insecticidal efficiency and poor degradability. Pyrethroid isomers with low insecticidal efficiency means that more pyrethroids are needed to achieve the expected insecticidal effects. Pyrethroid isomers with poor degradability can remain for an extended period in the environment and thus, can cause persistent harm to organisms in the environment. Consequently, using pyrethroids with high insecticidal efficiency and good degradability is environmentally friendly[13]. A specific environment may cause interconversions between different pyrethroid isomers, increasing or decreasing their degradability and insecticidal efficiency. CP [(RS)-R-cyano-3-phenoxybenzyl-(1RS)-cis, trans-3-(2,2-dichlorovinyl)-1, 1-dimethycyclopropanecarboxylate] contains four pairs of diastereomers, which are a pair of high-efficiency cis-CP (1S-cis-αR, 1R-cis-αS), high-efficiency trans-CP (1S-trans-αR, 1R-trans-αS), low-efficiency cis-CP (1R-cis-αR, 1S-cis-αS) and low-efficiency trans-CP (1R-trans-αR, 1S-trans-αS), and the two conformations they contain are considered as enantiomers. It is considered that the low-efficiency trans-CP and the high-efficiency trans-CP belong to trans-CP while the others belong to cis-CP. High-efficiency trans-CP and high-efficiency cis-CP belong to high-efficiency CP while the others belong to low-efficiency CP. In the natural environment, high-efficiency CP is readily converted into low-efficiency CP[14], and cis-CP is more difficult to decompose than trans-CP[15,16].

Oysters are widely consumed since they are high in protein, n-3 polyunsaturated fatty acids, essential amino acids, and

desirable[17]. Oysters are a filter-feeding aquatic animal living in the shallow sea, they filter massive amounts of seawater every day, thus, ingesting huge amounts of pollutants, such as microorganisms, heavy metals, microplastics, and pesticides[18,19]. These pollutants are subsequently absorbed by the human body when humans eat oysters, thus, threatening human health. CP and FP, hereinafter referred to as the pyrethroids, are potential contaminants in aquatic products such as oysters, hence, they need attention. However, there is no standard to limit the content of pyrethroids in aquatic products.

Cooking may destroy some nutrients from oysters. However, cooking also helps to eliminate or reduce many health-threatening contaminants[20,21]. Very little is currently known about the effects of cooking on pyrethroids in oysters. In addition, the content of pyrethroids in the food consumed is not necessarily equal to the amount of these toxic substances absorbed by the human body. Part of the pyrethroids are absorbed by the human body, and part are decomposed and discharged during digestion and subsequently excretion. Strangely, few studies have been conducted on the digestibility and absorption of pyrethroids from the food matrix.

Oysters are rich in proteins, and pyrethroids often accumulate in proteins. Different pyrethroids have different binding efficiency to proteins. However, very little is currently known about the release of different pyrethroids from proteins during digestion. We hypothesized that the isomers and concentration of CP and FP vary during digestion under different cooking methods.

Thus, the purposes of this study were to: (1) evaluate the binding degree of CP and FP to raw, steamed, and roasted oysters; (2) determine the changes of CP isomers during simulated digestion of raw, steamed, and cooked oysters; (3) evaluate the changes in the concentration of CP and FP during simulated digestion of raw, steamed, and roasted oysters; (4) assess the binding effects of CP and FP to oyster actin.

MATERIALS AND METHODS

Materials and reagents

Oyster samples (120–140 g each) were collected from the oyster breeding base located in Rushan City, Shandong Province, China, and transported to the laboratory quickly to maintain high physiological activity. Oyster actin was prepared and purified based on the method of Pardee & Spudich[22]. Fenpropathrin pesticide was purchased from Well-done Chemical Co., Ltd (Hangzhou, Zhejiang, China). Cypermethrin pesticide was purchased from Green Agricultural and Technology Group Co., Ltd (Beijing, China). Seawater crystals were purchased from Hai Sheng Seawater Crystal Factory (Tianjin, China). Acetonitrile (chromatographic grade), N-hexane (chromatographic grade), dimethyl sulfoxide (chromatographic grade), pepsin (P110927), and lipase A (L299012) were purchased from Aladdin Co., Ltd (Shanghai, China). Bile salt (B8210) was purchased from Solarbio Co., Ltd (Beijing, China). Porcine trypsin (P7545), cypermethrin standard, and fenpropathrin standard were purchased from Sigma-Aldrich Co., Ltd (Milwaukee, WI, USA). The MQ3-3 QuEChERS commercial kits were purchased from Shandong Qingyun Experiment Material Co., Ltd (Yantai, Shandong, China). All other chemicals of analytical reagent grade were purchased from Sinopharm Chemical Reagent Co., Ltd (Shanghai, China).

Artificially-contaminated oyster preparation

A total of six groups of oysters were artificially contaminated, the three groups were exposed to CP, and the other three groups were exposed to FP. Sixty litres of artificial seawater was formulated with distilled water and seawater crystals for each artificially-contaminated oyster group. Salinity (27.0% ± 1.0%) and temperature (26.0 ± 1.0 °C) were maintained throughout the whole experiment. The CP and FP pesticides were separately diluted to 1 g·L^{-1} in dimethyl sulfoxide. The diluent was then poured into each artificial seawater set up, maintaining the pyrethroids concentration to 166.67 μg·L^{-1}. Fresh oysters (7.5 kg) were fed in each 60 L of artificially contaminated seawater for 30 h. The artificially contaminated oysters were sacrificed and stored at −20 °C for further analysis. The storage time was less than four weeks to avoid the decomposition of absorbed pyrethroids and oyster matrix denaturation.

Cooking methods of oysters

The oysters, CP-, and FP-contaminated, were divided into three groups according to the intended treatment: a) raw (i.e., oysters without any heating), b) steamed (i.e., water in a steamer was heated to boiling, and then oysters with complete shells were steamed for 5 min until the shells opened), and c) roasted (i.e., the oven was preheated at 200 °C for 5 min, oysters with the shells on were roasted in the oven for 20 min). The cooking loss of the oyster meat was calculated following the method of Tobin et al.[23] as follows: Cooking loss rate (%) = weight difference of oyster meat before and after cooking (g)/weight of oyster meat before cooking (g) × 100%.

The oyster meat was separated from the shells, homogenized to a paste using a blender (JY-200B, Zhongshan Jiuyuan Electric Appliance Co., Ltd; Zhongshan, China), and stored for further analysis.

In vitro simulated digestion model

The *in vitro* simulated digestion model was established to assess the changes to CP and FP in oyster meat during digestion. This model was based on the conceptual framework proposed by Brodkorb et al.[24], and some improvements were made according to the conditions of this study. In brief, a stable temperature horizontal shaking bath (THZ-82, Jiangsu JieRuiEr Electric Appliances Co., Ltd; Changzhou, China) was used to simulate the digestive and gastrointestinal peristalsis temperature (37 °C) and medium oscillation speed was maintained. Pepsin, lipase A, porcine trypsin, and bile salt were used in this model. Salivary amylase was not added in the oral phase because the price was high, and oysters contain low levels of starch. A small intestinal buffer phase was maintained in this model to simulate the gastric emptying process.

The whole simulated digestion process was carried out as follows: oral phase (5 g oyster meat paste was equally diluted with simulated salivary fluid, and the digestion process lasted 2 min, the final pH was 7.0 ± 0.2), gastric phase (oral bolus was equally diluted with simulated gastric fluid, and the digestion process lasted 150 min), small intestinal buffer phase (the same amount of simulated intestinal fluid was slowly added to the gastric chyme within 15 min, the final pH was 8.0 ± 0.2), small intestinal phase (the digestion process lasted 120 min after the small intestinal buffer phase). During the gastric phase, 5 M HCl was added gradually to simulate a gradual pH decrease (0.08 mL HCl was added at the beginning of the gastric phase, and then 0.04 mL HCl was added every quarter until 0.4 mL HCl was

ultimately added to the gastric chyme)[25]. The pH of the buffer system during the simulated gastric phase is shown in Fig. 1. A pH polynomial fitting curve was fitted based on the method of Sams et al., and it was slightly lower than the pH of the solid-liquid meal during the actual gastric phase recorded by Sams et al.[26], which might be due to oyster meat paste having a lower buffering effect on pH than the solid-liquid meal.

CP and FP extraction

The extraction of CP and FP from oyster meat paste was based on the method of Jiao et al.[27]. CP and FP were extracted by MQ3-3 QuEChERS commercial kits, which mainly consisted of an extraction tube, a salt package, and a purification pipe. The sampling rules for sample collections at different digestion stages were as follows: for the oyster meat paste before digestion, 5 g was collected; for the gastric chyme, the samples were taken and centrifuged immediately every 30 min from the beginning of the gastric phase, then 10 mL supernatant was collected; for the small intestinal chyme, the samples were taken and centrifuged immediately every 30 min from the beginning of the small intestinal phase, then 15 mL supernatant was collected. Sampling was repeated three times, and the samples were immediately transferred into an extraction tube with 5 mL ultrapure water and mixed for 1 min. Fifteen milliliters acetonitrile containing 1% acetic acid was added to the extraction tube and mixed for 1 min. Subsequently, the salt bag was added to the extraction tube and mixed for 3 min to extract the target compounds fully. The mixture was centrifuged at 2,930× g for 3 min and the supernatant (5 mL) was collected in a purification pipe and mixed for 1 min. The mixture was filtered through a membrane filter (Nylon, 0.22 μm), 3 mL of the filtrate was taken, flushed to dryness with nitrogen at 45 °C, and then redissolved in 2 mL N-hexane.

CP and FP determination using GC-ECD

CP and FP determination was performed using an Agilent 7890B gas chromatography system equipped with an ECD detector. Chromatographic separation was carried out using an HP-5 capillary column (30 m × 0.320 mm × 0.25 μm film thickness; Agilent, USA). Injection port and detector temperatures were maintained at 250 and 300 °C, respectively. The oven temperature was maintained at 160 °C for 1 min, followed by a temperature ramp at 20 °C/min to 215 °C, held for 1 min, ramped up by 0.5 °C/min to 220 °C, held for 1 min, and finally ramped up at 0.1 °C/min to 222 °C, and held for 20 min. The nitrogen carrier gas was maintained at a flow rate of 1.0 mL·min^{-1}. A 1 μL sample was injected in splitless mode.

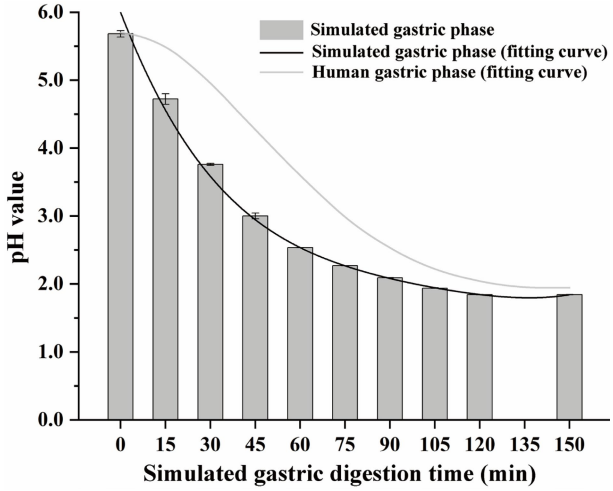

Fig. 1 The pH relates to the simulated gastric phase and human gastric phase. The fitting curve of human gastric phase pH refers to the conclusion of Sams et al.[26]

Fluorimetric titration

Fluorimetric titration was carried out to quantitatively analyze the interaction between CP and FP with oyster actin. CP and FP standards were dissolved in 0.5% dimethyl sulfoxide solution at concentrations of 2.40 mM (CP) and 2.86 mM (FP), respectively. Oyster actin stock solution (2.21 × 10^{-6} M) was prepared in 0.02 M Tris-HCl buffer (pH 8.0) containing 0.2 M NaCl. 0.9 mL oyster actin stock solution was added to quartz cuvettes, 1 cm path length. CP and FP solutions were successively added to the cuvettes separately with a trace syringe, and the fluorescence spectrum was scanned immediately after each addition. The final concentrations of CP and FP were 121.52 and 74.29 nM, respectively. The fluorescence titration was repeated three times.

The fluorescence intensity of the mixtures was measured by a spectrofluorometer (F-4500, Hitachi, Japan) equipped with a 150 W xenon lamp and a thermostat bath. The parameters were set as follows: the temperature was 298 K; the excitation wavelength was 280 nm; the emission wavelength range was 290–450 nm, and the excitation and emission slit width were both 5.0 nm.

Isothermal titration calorimetry

Isothermal titration calorimetry (ITC) was carried out to measure the enthalpy changes of CP and FP binding to oyster actin at 298 K by a microcalorimeter (Nano ITC, TA Instruments, USA). A 200 μL sample of oyster actin stock solution (2.21 × 10^{-6} M) was degassed and loaded into sample cells. CP and FP standards, 142.73 μM (CP) and 142.66 μM (FP), respectively, were separately prepared in 0.5% dimethyl sulfoxide, degassed, and then loaded into reference cells. CP and FP solutions (2.5 μL of each) were separately injected into the oyster actin stock solution 20 consecutive times by a rotating syringe. The rotating speed of the injector was 300 rpm and the injection interval was 200 s.

Statistical analysis

The results were expressed as mean ± standard deviation. Statistical analysis was carried out using IBM SPSS Statistics 26 (IBM Corp., USA). One-way ANOVA was carried out and means were considered significant at $p < 0.05$. The thermodynamic parameters between oyster actin and CP and FP were obtained using the NanoAnalyze software, and the fitting method was multi-point fitting. The operative quenching mechanism of CP/FP-oyster actin was deduced by the Stern–Volmer equation[28]:

$$\frac{F_0}{F} = 1 + K_{SV}[Q] = 1 + K_q\tau_0[Q]$$

where F_0 is the fluorescence intensities of oyster actin without CP or FP; F is the fluorescence intensities of oyster actin under the influence of CP or FP; K_{SV} is the Stern–Volmer dynamic quenching constant; [Q] is the concentration of CP or FP; K_q is the quenching rate constant of oyster actin; τ_0 is the average lifetime of the fluorophore without quencher, $\tau_0 = 10^{-8}$ s.

RESULTS AND DISCUSSION

QuEChERS recovery of CP and FP with different cooking methods

There were four peaks of CP with retention times of 46.1 min (low-efficiency cis-CP), 48.0 min (low-efficiency trans-CP), 49.0 min (high-efficiency cis-CP), and 49.8 min (high-efficiency trans-CP). The diastereomers of CP can be separated while the enantiomers of CP cannot be separated through appeal chromatographic conditions (Fig. 2). There was one peak of FP with a retention time of 21.8 min. FP contains a pair of enantiomers that cannot be separated through appeal chromatographic conditions (Fig. 2).

The concentrations of CP and FP changed significantly ($p < 0.05$) with different cooking methods. The cooking losses of oysters were 33.92% (steamed) and 42.13% (roasted), respectively. The QuEChERS recovery of CP from oyster meat was 0.469 $\mu g \cdot g^{-1}$ (raw), 0.639 $\mu g \cdot g^{-1}$ (steamed), and 1.085 $\mu g \cdot g^{-1}$ (roasted), and that of FP was 0.212 $\mu g \cdot g^{-1}$ (raw), 0.543 $\mu g \cdot g^{-1}$ (steamed), and 0.570 $\mu g \cdot g^{-1}$ (roasted), respectively (Fig. 3). Cooking can denature biological macromolecules in oysters, and can also attenuate the binding capacity of pyrethroids to biological macromolecules. Both CP and FP were easily extracted by organic solvents, and the QuEChERS recovery rate of CP and FP increased. It was observed that the binding capacity of both CP and FP to oyster tissue decreased

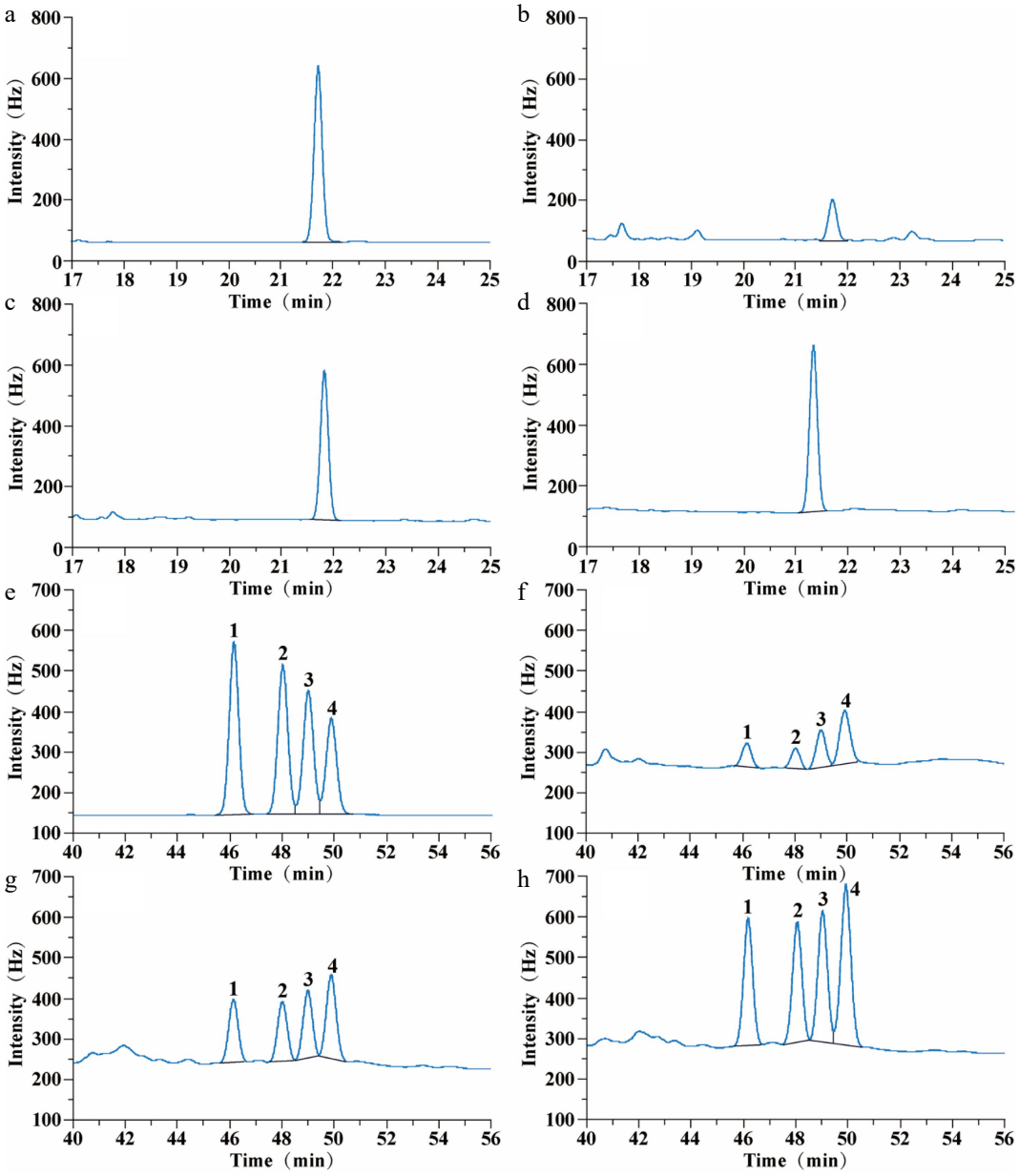

Fig. 2 Gas chromatograms of FP and CP from raw, steamed, and roasted oyster meat: (a) 0.5 $\mu g \cdot mL^{-1}$ FP standard chromatogram; (b) FP chromatogram of raw oysters; (c) FP chromatogram of steamed oysters; (d) FP chromatogram of roasted oysters; (e) 1 $\mu g \cdot mL^{-1}$ CP standard chromatogram; (f) CP chromatogram of raw oysters; (g) CP chromatogram of steamed oysters; (h) CP chromatogram of roasted oysters. The FP retention time was 21.8 min. CP retention time was 46.2 min (Low-efficiency cis-CP, peak 1); 48.0 min (Low-efficiency trans-CP, peak 2); 49.0 min (High-efficiency cis-CP, peak 3), and 49.8 min (High-efficiency trans-CP, peak 4).

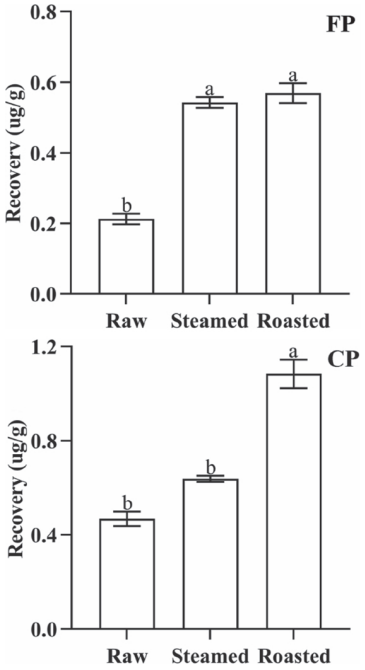

Fig. 3 QuEChERS recovery of FP and CP from 1 g oyster meat exposed to different cooking methods (steamed and roasted). Raw was uncooked. (Same lowercase letters (a, b) indicate no significant (ANOVA, $p > 0.05$) difference between the two groups of data).

significantly ($p < 0.05$) after roasting. In contrast, there was an insignificant ($p > 0.05$) change in the binding capacity of CP to steamed oyster tissues, while the binding capacity of FP to steamed oyster tissue decreased significantly ($p < 0.05$). The differences in the changes in binding capacity can be attributed to the different parameters of the cooking methods (such as temperature, cooking time, and other specific operations in cooking) associated with the different cooking methods tested.

Isomer changes of CP exposed to different cooking methods

The proportion of CP isomers changed significantly ($p < 0.05$) in both steamed and roasted oysters. The share of cis-CP isomers increased significantly ($p < 0.05$) after steaming and roasting, increasing from 43.74% (raw) to 46.64% (steamed) and 47.04% (roasted), respectively (Fig. 4). Previous studies indicated that high-efficiency CP and low-efficiency CP could interconvert with each other, but cis-CP and trans-CP cannot[14]. Cis-CP is more difficult to decompose than trans-CP *in vivo* or in the natural environment, and hence, cis-CP can cause more severe environmental and biological harm than trans-CP[15,16]. Our study indicated that the isomerization could be attributed to the fact that cis-CP and trans-CP are decomposed while high-efficiency CP and low-efficiency CP interconvert with each other. However, trans-CP is more susceptible to decomposition than cis-CP under the combined effect of oyster matrix and high temperature.

The percentage share of high-efficiency CP decreased significantly ($p < 0.05$) after steaming and roasting, from 67.58% (raw) to 55.16% (steamed), and 55.11% (roasted) (Fig. 4). Previous research demonstrated that high-efficiency CP and low-efficiency CP can be interconverted *in vivo* or in the

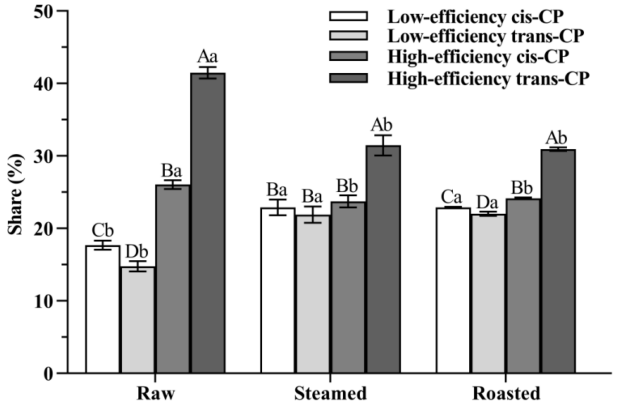

Fig. 4 The share of CP isomers is from oyster meat (raw, steamed, and roasted). Different uppercase letters represent differences in CP isomer shares from oyster meat with the same cooking methods (ANOVA, $p < 0.05$). Different lowercase letters represent differences in each pair of CP isomers from oyster meat with different cooking methods (ANOVA, $p < 0.05$).

natural environment[14]. Thus, it is possible that in this study, the high-efficiency CP of raw oysters was transformed into low-efficiency CP by steaming and roasting.

Isomer changes of CP during simulated digestion

As shown in Fig. 5, the changes in the proportion of CP isomers in contaminated raw, steamed, and roasted oysters during simulated digestion were more similar. The share of high-efficiency trans-CP increased initially and then decreased at the end of the digestion period, while the shares of the other isomers decreased initially and then increased at the end of the digestion period. The change in the share of trans-CP was more significant ($p < 0.05$) than that of cis-CP in the whole simulated digestion process, especially for the high-efficiency trans-CP, the percentage share of high-efficiency trans-CP increased suddenly in the small intestinal buffer phase. This phenomenon can be explained by trans-CP being easier to decompose than cis-CP, and cis-CP binds more firmly to oyster tissues than trans-CP; high-efficiency CP and low-efficiency CP can transfer to each form during pH variation. Similar studies also demonstrated that cis-CP was more difficult to decompose than trans-CP by mammalian hepatic carboxylesterases *in vivo*[29]. The cis structure of CP makes the carbonyl carbon of CP difficult to contact with the enzyme active site, but the trans structure makes the process easier[30]. Thus, cis-CP can exist longer in the human body than trans-CP and can result in longer-term effects in the body. It is presumed that some digestive enzymes in the small intestine are similar to mammalian hepatic carboxylesterases, they can decompose trans-CP more quickly than cis-CP.

There were minor differences in the changes of CP isomers treated with different cooking methods, especially high-efficiency trans-CP. In the raw oyster group, the percentage share of high-efficiency trans-CP increased rapidly at the beginning of the gastric phase and decreased rapidly in the middle of the small intestinal phase, and the percentage share of high-efficiency trans-CP maintained a high level throughout the simulated digestion period, longer than the steamed and roasted groups. The percentage share of trans-CP was 56.26% (raw), 53.36% (steamed), and 52.96% (roasted) before

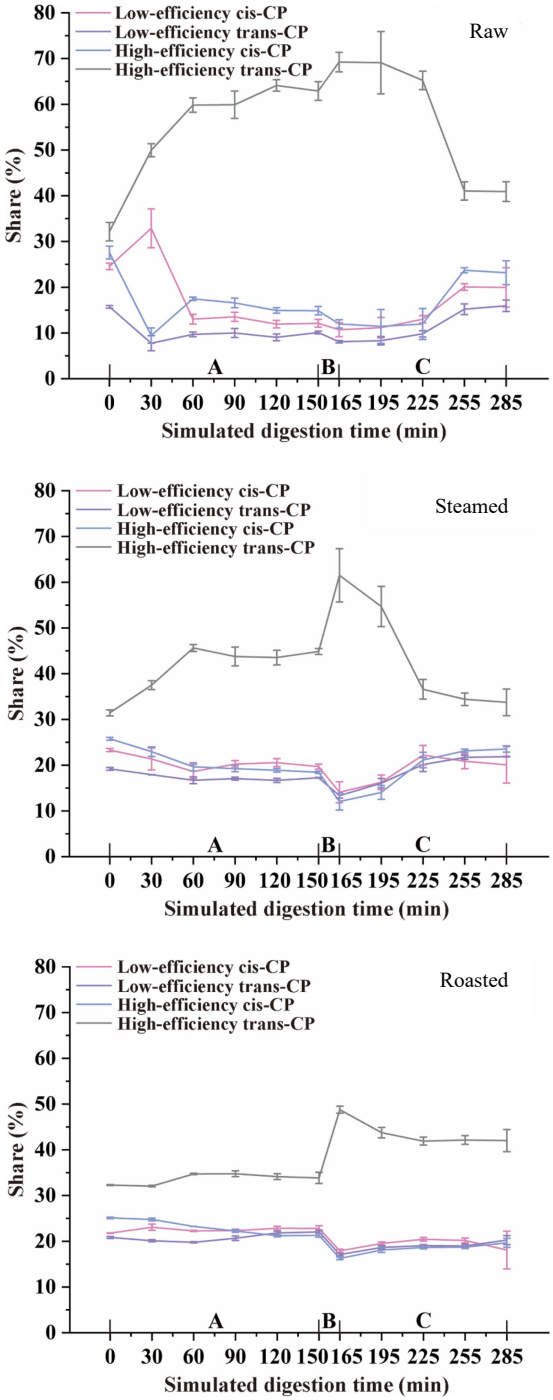

Fig. 5 CP isomers transformation during simulated digestion of raw, steamed, and roasted oysters. A, Gastric phase; B, Small intestinal buffer phase; C, Small intestinal phase.

simulated digestion but changed to 56.86% (raw), 55.63% (steamed), and 62.26% (roasted) at the end of the small intestinal phase. The percentage share of trans-CP changed insignificantly ($p > 0.05$) during simulated digestion of the raw group, while in streamed and roasted oysters it changed significantly ($p < 0.05$) after simulated digestion. Trans-CP is more environmentally friendly than cis-CP, and our results indicated that steaming and roasting may decrease pyrethroid toxicity after digestion. However, the decomposition products of CP are more concerning because some of them are more stable than CP and have a more hazardous effect on human health[31,32].

The change of CP and FP concentration during simulated digestion

As shown in Fig. 6, the concentration of CP during simulated digestion remained fairly constant in all oyster groups, raw, steaming, and roasting. A significant decrease ($p < 0.05$) in CP levels was observed in the initial gastric phase but with the progression of the gastric phase, CP levels increased gradually. However, the CP levels decreased sharply and significantly ($p < 0.05$) at the end of the gastric phase. The decline in CP levels in the initial stage of the gastric phase can be attributed to the weak enzyme activity in the low acid environment[33]. The rate of CP dissolution from the tissues is lower than the rate of CP decomposition from the digested liquids. With the continuation of the gastric phase, the enzyme activity rises, and CP is gradually released from tissues, thus raising the concentration of CP in the mixture. The dissolution rate of CP from the oyster meat paste began to decrease at the end of the gastric phase, and the low pH and high enzyme activity environment accelerated the decomposition of CP, making the rate of CP decomposition from digested liquids higher than the rate of CP dissolution from the tissues.

The concentration of CP decreased significantly ($p < 0.05$) with simulation intestinal fluid added. However, with the rapid changes in pH and the addition of intestinal digestive enzymes, a huge amount of CP was released during the small intestinal

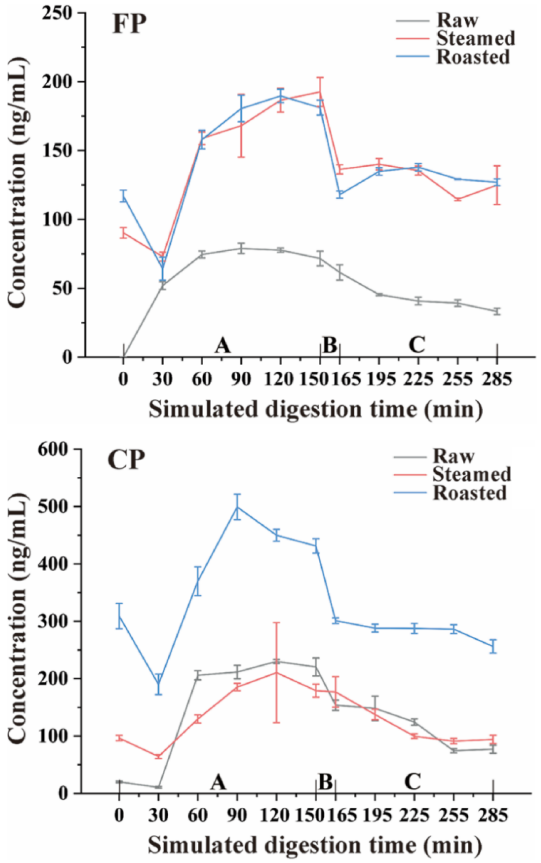

Fig. 6 CP and FP concentration change tendency during simulated digestion after different cooking methods (steamed and roasted). Raw was uncooked. A, Gastric phase; B, Small intestinal buffer phase; C, Small intestinal phase.

buffer phase. The level of CP decreased significantly ($p < 0.05$) in the small intestinal phase, which can be attributed to CP being decomposed severely by the simulated intestinal fluid, especially pancreatic and bile juices because of their strong digestive ability.

The change in the concentration of FP during simulated digestion was similar to that of CP. However, the dissolution of FP in the raw group was much lower than that of steamed and roasted groups in the initial phase of gastric digestion. This phenomenon can indicate two possible hypotheses, i.e., (1) that the polarity of FP is weaker than that of CP, and the dissociation of FP is much slower in aqueous solution than that of CP, and (2) that cooking can promote the dissociation of pyrethroids from meat tissues.

The amounts of CP and FP released from oyster meat paste changed significantly ($p < 0.05$) during simulated digestion. The amounts of CP released were 0.617 μg·g^{-1} (raw), 0.498 μg·g^{-1} (steamed), and 1.186 μg·g^{-1} (roasted), and that of FP were 0.266 μg·g^{-1} (raw), 0.660 μg·g^{-1} (steamed) and 0.588 μg·g^{-1} (roasted) at the end of the simulated digestion process (Fig. 7). The amount of CP and FP released from roasted oyster meat increased significantly ($p < 0.05$) at the end of the simulated digestion period. However, the amount of FP released from oyster tissues increased significantly ($p < 0.05$) at the end of the digestion when oysters were steamed, while that of CP showed the opposite trend. Our results indicated that different cooking methods can cause completely different effects on different pyrethroids.

Fluorescence titration of oyster actin with CP and FP

Oyster actin had a strong fluorescence emission peak at 338 nm after excitation at 280 nm. With the addition of CP and FP, the fluorescence intensity of oyster actin decreased significantly ($p < 0.05$) with a slight blue shift, but the decrease in fluorescence intensity of oyster actin slowed down (Fig. 8). The blue shift in the emission maxima can be attributed to the increase in hydrophobicity around the fluorophore(s). The decrease in the fluorescence intensity of oyster actin indicated that CP and FP can interact with oyster actin forming non-fluorescent complexes, thus, changing the three-dimensional structure conformation of oyster actin and quenching its intrinsic fluorescence.

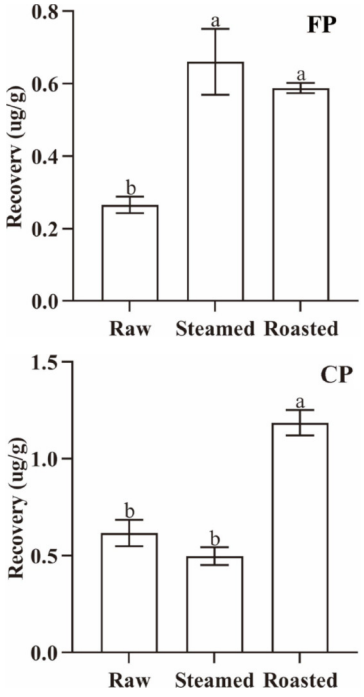

Fig. 7 The amount of released FP and CP from 1 g oyster meat at the end of simulated digestion with different cooking methods (steamed and roasted). Raw was uncooked. (Same lowercase letters (a-b) indicate no significant (ANOVA, $p > 0.05$) difference between the two groups of data).

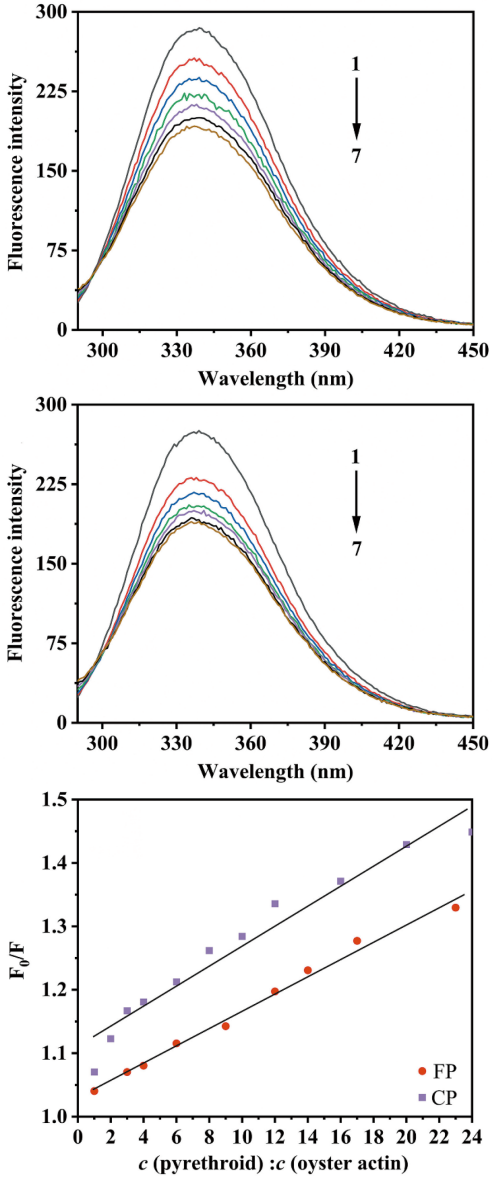

Fig. 8 (a) The fluorescence quenching spectra of oyster actin in the presence of FP, c (FP: oyster actin) = 0, 6:1, 12:1, 17:1, 23:1, 29:1, 35:1 for curves 1–7, respectively. (b) The fluorescence quenching spectra of oyster actin in the presence of CP, *c* (CP: oyster actin) = 0, 10:1, 19:1, 29:1, 39:1, 48:1, 58:1 for curves 1–7, respectively. (c) Effects of CP and FP concentrations on the fluorescence quenching of oyster actin at 338 nm, where F_0 is the fluorescence intensities of oyster actin without CP or FP; F is the fluorescence intensities of oyster actin under the influence of CP or FP; *c* (pyrethroid) : *c* (oyster action) is the molar ratio of CP or FP to oyster actin.

The Stern–Volmer dynamic quenching constant (K_{sv}) and quenching rate constant (K_q) were calculated by the Stern-Volmer equation, and the fitting curve is shown in Fig. 8. With oyster actin concentration of 2.21 μM, the K_q of CP was 3.51×10^{12} L·mol^{-1}·s^{-1}, and that of FP was 2.18×10^{12} L·mol^{-1}·s^{-1} and higher than the dynamic quenching constant (2×10^{10} L·mol^{-1}·s^{-1}). This indicated that ground state complexes were formed between CP or FP and the oyster actin, and static quenching was generated[34]. The K_{sv} reflects the binding ability of CP and FP to oyster actin. In the case of static quenching, the K_{sv} of CP to oyster actin (3.51×10^4 L·mol^{-1}) was larger than that of FP (2.18×10^4 L·mol^{-1}), possibly indicating that CP binds stronger to oyster actin than FP. This could explain the higher retention and lower recovery of CP during simulated digestion compared with FP.

Binding thermodynamics of CP and FP to oyster actin

ITC can accurately depict the binding and thermodynamic parameters, indicating the interaction forces between the pyrethroids and oyster actin, including electrostatic interactions, hydrogen bond formation, hydrophobic interactions, van der Waals interactions, steric contacts, and so on. With the gradual addition of CP and FP to oyster actin, the size of the peak generated decreased and reached saturation due to the combination of CP and FP with oyster actin (Supplemental Fig. S1).

The binding and thermodynamic parameters were calculated by the raw heat data of the ITC (Table 1). The positive binding enthalpy and entropy indicated that hydrophobic interactions were a major force between CP or FP and oyster actin[35]. The negative Gibbs free energy suggested that the binding of CP and FP to oyster actin was a spontaneous process, and that oyster actin can accumulate pyrethroids spontaneously in the natural environment (the other biological macromolecules in oysters can be having a similar phenomenon)[36]. The CP and FP enriched in oyster actin needed additional energy to be separated and were difficult to separate in a natural water environment, which made the concentrations of CP and FP in oyster actin rise above that in the aquaculture water. However, these CP and FP enriched in oyster actin can be released with the destruction of the binding sites between oyster actin and pyrethroids during digestion. The association constant of CP to oyster actin was significantly higher ($p < 0.05$) than that of FP, indicating a high affinity to oyster actin, which can help to explain that oysters accumulated more CP than FP under the same exposure condition.

Table 1. Binding and thermodynamic parameters of oyster actin and CP or FP obtained from ITC.

Parameter		FP	CP
K_a (association constant, M^{-1})	K_{a1}	7.12×10^4	1.09×10^7
	K_{a2}	2.84×10^4	8.20×10^5
n (binding stoichiometry)	n_1	7.83	3.43
	n_2	10.00	12.41
ΔH (binding enthalpy, J·mol^{-1})	ΔH_1	2.00×10^5	7.17×10^4
	ΔH_2	2.00×10^5	2.57×10^4
ΔS (entropy, J·mol^{-1}·K^{-1})	ΔS_1	7.64×10^2	3.75×10^2
	ΔS_2	7.56×10^2	2.00×10^2
ΔG (Gibbs free energy, J·mol^{-1})	ΔG_1	-2.77×10^4	-4.01×10^4
	ΔG_2	-2.25×10^4	-3.39×10^4

CONCLUSIONS

Our study demonstrated that different cooking methods (raw, steaming, and roasting) affected the binding of CP and FP to oyster tissues and their release from oyster tissues during digestion. CP and FP could interact with oyster actin spontaneously in the natural environment and change its three-dimensional structure conformation. CP bound stronger to oyster actin than FP, and oysters accumulated more CP than FP under the same exposure conditions. Different cooking methods affected the specific changes of CP isomers during simulated digestion, but the final proportion of CP isomers at the end of simulated digestion was less affected.

ACKNOWLEDGMENTS

The research was supported by the National Key R&D Program of China (2019YFD0901704).

Conflict of interest

The authors declare that they have no conflict of interest.

Dates

Received 3 August 2022; Accepted 8 December 2022; Published online 31 January 2023

REFERENCES

1. Saillenfait AM, Ndiaye D, Sabaté JP. 2015. Pyrethroids: Exposure and health effects - An update. *International Journal of Hygiene and Environmental Health* 218:281–92
2. Tang W, Wang D, Wang J, Wu Z, Li L, et al. 2018. Pyrethroid pesticide residues in the global environment: An overview. *Chemosphere* 191:990–1007
3. Li HZ, Cheng F, Wei YL, Lydy MJ, You J. 2017. Global occurrence of pyrethroid insecticides in sediment and the associated toxicological effects on benthic invertebrates: An overview. *Journal of Hazardous Materials* 324:258–71
4. Weston DP, Holmes RW, You J, Lydy MJ. 2005. Aquatic toxicity due to residential use of pyrethroid insecticides. *Environmental Science and Technology* 39:9778–84
5. Fabro L, Varca LM. 2012. Pesticide usage by farmers in Pagsanjan-Lumban catchment of Laguna de Bay, Philippines. *Agricultural Water Management* 106:27–34
6. Stehle S, Schulz R. 2015. Agricultural insecticides threaten surface waters at the global scale. *PNAS* 112:5750–55
7. Paul EA, Simonin HA. 2006. Toxicity of three mosquito insecticides to crayfish. *Bulletin of Environmental Contamination and Toxicology* 76:614–21
8. Qi X, Zheng M, Wu C, Wang G, Feng C, et al. 2012. Urinary pyrethroid metabolites among pregnant women in an agricultural area of the Province of Jiangsu, China. *International Journal of Hygiene and Environmental Health* 215:487–95
9. Wu C, Feng C, Qi X, Wang G, Zheng M, et al. 2013. Urinary metabolite levels of pyrethroid insecticides in infants living in an agricultural area of the Province of Jiangsu in China. *Chemosphere* 90:2705–13
10. Koureas M, Tsakalof A, Tsatsakis A, Hadjichristodoulou C. 2012. Systematic review of biomonitoring studies to determine the association between exposure to organophosphorus and pyrethroid insecticides and human health outcomes. *Toxicology Letters* 210:155–68

11. Pérez-Fernández V, García MA, Marina ML. 2010. Characteristics and enantiomeric analysis of chiral pyrethroids. *Journal of Chromatography A* 1217:968−89
12. Liu W, Gan J. 2004. Separation and analysis of diastereomers and enantiomers of cypermethrin and cyfluthrin by gas chromatography. *Journal of Agricultural and Food Chemistry* 52:755−61
13. Chang J, Xu P, Li W, Li J, Wang H. 2019. Enantioselective elimination and gonadal disruption of lambda-cyhalothrin on lizards (eremias argus). *Journal of Agricultural and Food Chemistry* 67:2183−89
14. Liu W, Qin S, Gan J. 2005. Chiral stability of synthetic pyrethroid insecticides. *Journal of Agricultural and Food Chemistry* 53:3814−20
15. Khazri A, Sellami B, Dellali M, Corcellas C, Eljarrat E, et al. 2016. Diastereomeric and enantiomeric selective accumulation of cypermethrin in the freshwater mussel *Unio gibbus* and its effects on biochemical parameters. *Pesticide Biochemistry and Physiology* 129:83−88
16. Li ZY, Zhang ZC, Zhang L, Leng L. 2008. Stereo and enantioselective degradation of β-Cypermethrin and β-Cyfluthrin in soil. *Bulletin of Environmental Contamination and Toxicology* 80:335−39
17. Venugopal V, Gopakumar K. 2017. Shellfish: nutritive value, health benefits, and consumer safety. *Comprehensive Reviews in Food Science and Food Safety* 16:1219−42
18. Cho Y, Shim WJ, Jang M, Han GM, Hong SH. 2019. Abundance and characteristics of microplastics in market bivalves from South Korea. *Environmental Pollution* 245:1107−16
19. Wang J, Koopman KR, Collas FPL, Posthuma L, de Nijs T, et al. 2021. Towards an ecosystem service-based method to quantify the filtration services of mussels under chemical exposure. *Science of the Total Environment* 763:144196
20. Saha S, Halder M, Mookerjee S, Palit A. 2020. Preponderance of multidrug-resistant, toxigenic, and thermotolerant enteropathogenic bacteria in raw and cooked seafood of indo-gangetic basin and associated health risks. *Journal of Aquatic Food Product Technology* 29:838−49
21. Alves RN, Maulvault AL, Barbosa VL, Cunha S, Kwadijk CJAF, et al. 2017. Preliminary assessment on the bioaccessibility of contaminants. of emerging concern in raw and cooked seafood. *Food and Chemical Toxicology* 104:69−78
22. Pardee JD, Aspudich J. 1982. Purification of muscle actin. *Methods in Enzymology* 85:164−81
23. Tobin BD, O'Sullivan MG, Hamill RM, Kerry JP. 2013. The impact of salt and fat level variation on the physiochemical properties and sensory quality of pork breakfast sausages. *Meat Science* 93:145−52
24. Brodkorb A, Egger L, Alminger M, Alvito P, Assunção R, et al. 2019. INFOGEST static in vitro simulation of gastrointestinal food digestion. *Nature Protocols* 14:991−1014
25. Minekus M, Alminger M, Alvito P, Ballance S, Bohn T, et al. 2014. A standardised static *in vitro* digestion method suitable for food - an international consensus. *Food and Function* 5:1113−24
26. Sams L, Paume J, Giallo J, Carrière F. 2016. Relevant pH and lipase for *in vitro* models of gastric digestion. *Food and Function* 7:30−45
27. Jiao YD, Liu CE, Feng CS, Regenstein JM, Luo YK, et al. 2021. Bioaccessibility and intestinal transport of deltamethrin in pacific oyster (*Magallana gigas*) using simulated digestion/NCM460 cell models. *Frontiers in Nutrition* 8:726620−31
28. Zhang G, Ma Y. 2013. Mechanistic and conformational studies on the interaction of food dye amaranth with human serum albumin by multispectroscopic methods. *Food Chemistry* 136:442−49
29. Nishi K, Huang H, Kamita SG, Kim IH, Morisseau C, et al. 2006. Characterization of pyrethroid hydrolysis by the human liver carboxylesterases hCE-1 and hCE-2. *Archives of Biochemistry and Biophysics* 445:115−23
30. Huang H, Fleming CD, Nishi K, Redinbo MR, Hammock BD. 2005. Stereoselective hydrolysis of pyrethroid-like fluorescent substrates by human and other mammalian liver carboxylesterases. *Chemical Research in Toxicology* 18:1371−77
31. Zhu Q, Yang Y, Lao Z, Zhong Y, Zhang K, et al. 2020. Photodegradation kinetics, mechanism and aquatic toxicity of deltamethrin, permethrin and dihaloacetylated heterocyclic pyrethroids. *Science of the Total Environment* 749:142106
32. Liu X, Wang P, Liu C, Liang Y, Zhou Z, et al. 2017. Absorption, distribution, metabolism, and in vitro digestion of beta-cypermethrin in laying hens. *Journal of Agricultural and Food Chemistry* 65:7647−52
33. Salelles L, Floury J, Le Feunteun S. 2021. Pepsin activity as a function of pH and digestion time on caseins and egg white proteins under static *in vitro* conditions. *Food and Function* 12:12468−78
34. Wang Y, Zhang G, Yan J, Gong D. 2014. Inhibitory effect of morin on tyrosinase: Insights from spectroscopic and molecular docking studies. *Food Chemistry* 163:226−33
35. Qi H, Wang Y, Wang X, Su L, Wang Y, et al. 2021. The different interactions of two anticancer drugs with bovine serum albumin based on multi-spectrum method combined with molecular dynamics simulations. *Spectrochimica Acta Part A: Molecular and Biomolecular Spectroscopy* 259:119809
36. Su H, Xu Y. 2018. Application of ITC-based characterization of thermodynamic and kinetic association of ligands with proteins in drug design. *Frontiers in Pharmacology* 9:1113